RSC Advances

ROYAL SOCIETY OF CHEMISTRY

www.rsc.org/advances

Graphical Abstract

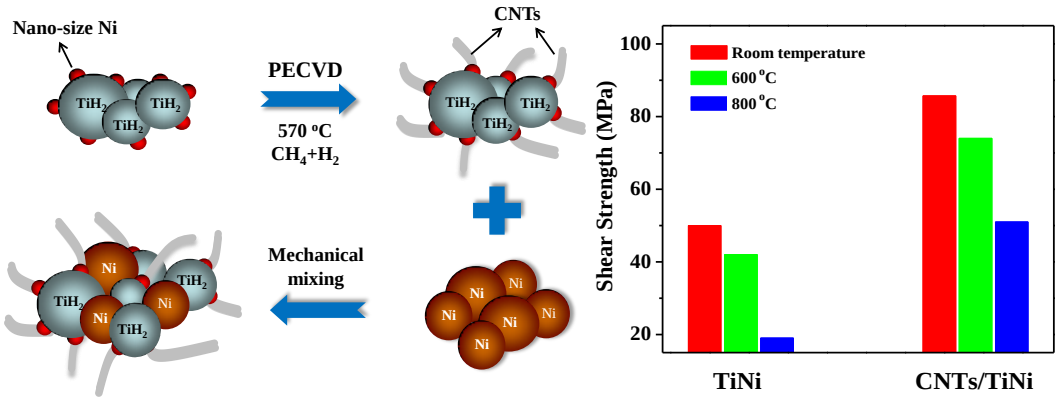

The CNTs played a key role in reducing residual stress and reinforcing mechanical properties (in both room and high temperature) of the brazed joint.

Joining of SiO_2-BN ceramic to Nb using CNTs-reinforced brazing alloy

Jun Lei Qi*, Jing Huang Lin, Yu Han Wan, Li Xia Zhang, Jian Cao, Ji Cai Feng*

State Key Laboratory of Advanced Welding and Joining, Harbin Institute of Technology, Harbin 150001, China

*Corresponding author: Tel. /fax: 86-451-86418146;

E-mail: jlqi@hit.edu.cn (J. L. Qi), fengjc@hit.edu.cn (J. C. Feng);

Abstract:

Brazing SiO_2-BN ceramic with Nb often meets the problems of high residual stress caused by the difference of the thermal expansion coefficients and poor mechanical properties under high temperature. To overcome these problems, here we developed a new type of carbon nanotubes (CNTs)-reinforced TiNi brazing alloys via an *"in-situ growth"* method by PECVD. The CNTs/TiNi brazing alloy has very homogeneously dispersed CNTs within the TiNi brazing alloys, which consists of *in-situ* growth of CNTs on the TiH_2 powders and Ni powders mixed evenly into the CNTs/TiH_2 powders. It can be applied in the brazing of SiO_2-BN and Nb. Results show that the addition of CNTs into TiNi brazing alloy is very beneficial for the dissolution and diffusion of Nb in the brazed joint, because it can promote more TiNi-(Nb,Ti) eutectics emerged in the most of brazing seam. Further, the average shear strengths of the brazed joint at room temperature are raised from 49 to 85 MPa with the 1.5vol.% CNTs added into TiNi brazing alloy. Especially, the brazed joint at 800 ^oC still has very high shear strength as 51 MPa, about 1.7 times stronger than that of TiNi brazing alloy. These results suggest that the CNTs played a key role in reducing residual stress and reinforcing mechanical properties (in both room and high temperature) of the brazed joint. It provides a way for the development of CNT-reinforced brazing alloy.

Key words: CNTs, reinforced, brazing, brazing alloy, high temperature properties

1. Introduction

Due to its unique combinations of various properties, such as low density, good mechanical and excellent thermal shock resistance, SiO_2-BN ceramic has potential applications in thermal protection parts.[1, 2] To extend the practical application of SiO_2-BN ceramic, it is essential to be able to join them to metallic components.[3, 4] For example, the assembly of nozzle components requires joining a SiO_2-BN ceramic nozzle to a metallic holder. However, joining of SiO_2-BN ceramic is a great challenge since most conventional methods are not suitable. The major challenge in joining SiO_2-BN ceramic to metals is not so much the chemical dissimilarity between materials but rather the stresses induced by the mismatch between the coefficients of thermal expansion (CTE) of the components that impairs the joint integrity.[4, 5] Considering its applications under high temperatures, the joint should possess good mechanical behavior. Therefore, it is essential to reduce or eliminate the residual stresses in the interfacial region to improve the joining quality and enhance the mechanical properties under high temperatures.

To overcome the inherent problems mentioned above, many studies suggested the addition of low CTE materials (such as ceramic fibers or particles) into brazing alloys to improve the mechanical properties (in both room and high temperature) of a ceramic-metal joint.[5-7] However, this method had its own limitations: high weight ratio, uneven distribution and non-wetting of the reinforcements, as well as non-controllability of brazing alloy reinforcement interfaces.[8, 9] Recently, Nai *et al.*[10-12] and Kumar *et al.*[13, 14] have studied the effect of carbon nanotubes (CNTs) addition on the tensile and mechanical properties of Sn-Ag-Cu (SAC) solder alloys. Their studies indicated that when some CNTs were added into the SAC solder alloy, the wettability and mechanical properties would be convincingly improved. CNTs are

widely known to possess great physical, low-density, thermal, electrical, and mechanical properties, which make them suitable for preparing novel composites. Due to their excellent properties, they are widely used as reinforcement materials.[15, 16] Compared with the traditional reinforcements, CNTs show great mechanical properties, especially under high temperature conditions.[17] Currently, Ti-based brazing alloys are widely used to braze ceramics and metals.[18] However, there are still several factors limiting us to take full advantage of CNTs-reinforced Ti-based brazing alloys, for instance: (i) difficulty in homogeneously dispersing the CNTs in the Ti-based brazing alloys, (ii) reaction between CNTs and Ti due to the incomplete structure of CNTs easy mutually reactive with Ti in brazing process,[19, 20] and (iii) the contamination of Ti source, such as oxidation and carbonization of Ti in the CNTs composite and the brazing process. Therefore, overcoming these problems is a key to the realization of CNTs-reinforced brazing alloy used in ceramics and metals brazing.

To overcome these problems, here we report a new type of CNTs reinforced TiNi brazing alloys via an *"in-situ growth"* method using plasma enhanced chemical vapor deposition (PECVD). The obtained CNTs/TiNi brazing alloy was used to braze SiO_2-BN ceramic to Nb. The investigation emphasizes the effect of CNTs on the microstructures and shear strength of the brazed joints. Further, the strengthening mechanism of the CNTs by reducing residual stress and reinforcing mechanical properties of the brazed joint is also elucidated.

2. Experimental

The synthesis process of CNTs/TiNi brazing alloy is shown in Fig. 1. In order to prevent the contamination of Ti source, TiH_2 was selected as the Ti sources of CNTs/TiNi brazing alloy. Due to the hydrogen-bond in TiH_2, the reaction between Ti and C could be inhibited. Thus, CNTs/TiNi brazing alloy will effectively avoid being

contaminated in the synthesis process. CNTs/TiNi brazing alloy was synthesized by PECVD, using Ni nanoparticles as catalyst. The fabrication of Ni catalyst nanoparticles has been reported previously.[21, 22] The synthesis process of CNTs/TiNi brazing alloy mainly consists of three steps. The first step is to produce $Ni(NO_3)_2$-TiH_2 powders. $Ni(NO_3)_2 \cdot 6H_2O$ (99.9% purity) and TiH_2 (99.7% purity) were mixed in ethanol solution with constant stirring, and then the solution was heated up to obtain fine $Ni(NO_3)_2$-TiH_2 powders, which were employed in the following synthesis experiments. In the second step, the $Ni(NO_3)_2$-TiH_2 powders were kept in a quartz boat and placed at the same horizontal level in a PECVD reaction chamber.[21] The PECVD chamber was evacuated to a pressure below 5 Pa by a rotary pump, and then the chamber was maintained at 200 Pa with H_2 at a flow rate of 20 sccm. Since the decomposition temperature of TiH_2 is about 600 ^oC, [23] CNTs were grown at 570 °C for 15min by introducing a mixture of CH_4/H_2 into the reactor at a flow rate of 40/10 sccm. In the final step, the prepared CNTs/TiH_2 powders were mechanically mixed with Ni powders to form CNTs/TiNi brazing alloy.

The Nb substrate and SiO_2-BN ceramic were sandwiched between TiNi and CNTs/TiNi brazing alloy. After that the assembly was put into a vacuum furnace and a normal pressure (about 0.01MPa) was applied to maintain the close contact of the assembly. During the brazing process, the assembly was heated to 1140 ^oC at a rate of 15 ^oC/min. After being isothermally held at 1140 ^oC for 5min, the assembly was cooled down to room temperature at a rate of 5 ^oC/min without power.

The morphology and structure of the samples were characterized using scanning electron microscope (SEM) equipped for electron-dispersive spectroscopy (EDS), transmission electron microscopy (TEM), X-ray diffraction (XRD) and Raman spectroscopy. The shear strengths were also tested at both room and high temperatures.

At least five specimens were tested for each experimental condition.

3. Results and Discussion

Corresponding to the formation process as shown in Fig. 1, Fig. 2a-d show the SEM images of TiH_2, CNTs/TiH_2 and CNTs/TiH_2-Ni particles. The surface of pure TiH_2 particles is smooth and clean, as shown in Fig. 2a. Fig. 2b shows a low-magnification SEM image of CNTs *in-situ* grown on TiH_2 powders. The CNTs with the length in the range of 3~4 μm are homogeneously and densely distributed on the surface of TiH_2 powders. The CNTs on TiH_2 particles are not agglomerated and very similar at different regions, and their diameter and length are similar, as shown in Fig. 2b. Moreover, it can be observed that the CNTs are homogeneously dispersed into the TiH_2 powders. As shown in the inset of Fig. 2c, the as-grown CNTs show a typical tubular structure, where the surface of sidewalls is clean. After simply mechanically mixing with Ni powders, it can be found that the CNTs disperse homogeneously into the TiH_2-Ni powders, as shown in Fig. 2d. It can be clearly observed that the CNTs are not agglomerated at all, and network structures are formed between the CNTs and TiH_2-Ni powders. This result may be contributed to a certain binding force between the CNTs and TiH_2 particle since the CNTs are synthesized into the TiH_2 powders *in situ*. The morphology of the CNTs/TiH_2-Ni powders shows an ideal composite microstructure, displaying spherical morphologies with CNTs homogeneously dispersed into the powders.[21]

As a result, it demonstrates that the homogeneously dispersed CNTs within the TiH_2-Ni powders are achieved by the three-step procedure described above. Moreover, the most important feature of PECVD process is that the CNTs are synthesized into the TiH_2 powders in situ. It is also found that the density and length of the CNTs, or the CNTs' content of the composite powders can be easily tuned by adjusting the

experimental parameters, such as the growing time and the CH_4 percentage in mixture of CH_4/H_2 gases. With a shorter time and less CH_4 percentage, shorter and sparser CNTs can be obtained in the TiH_2 powders. Therefore, it is easy and practical to obtain different content of CNTs in CNTs/TiNi brazing alloy. In our case, CNTs' content in CNTs/TiNi brazing alloy is 1.5 vol.%.

Fig. 2e exhibits the XRD patterns of pure TiH_2, CNTs/TiH_2 and CNTs/TiH_2-Ni powders, and all diffraction peaks can be attributed. From XRD results (see Fig. 2e), it can be found the XRD peaks of pure TiH_2 powders (Black line in Fig. 1a) can be safely indexed to peak positions of $TiH_{1.924}$ with the face-centered cubic structure. [25] In the XRD pattern of CNTs/TiH_2 powders, a peak at 2θ=26.4° (Red line in Fig. 2e) is observed after the CNTs grown on TiH_2 powders compared with that of pure TiH_2. The peak at 2θ=26.4° can be assigned to graphite (002), which indicates that CNTs have been obtained and CNTs are mainly composed of well-crystallized graphite. [24] The other peaks can be indexed to peak positions of $TiH_{1.924}$. Furthermore, the peaks of TiC and TiO_2 do not appear in the XRD pattern. These results indicates that the TiH_2 does not decompose and maintains the original state in PECVD process, which further avoids the reaction between Ti and C, and prevents the contamination of Ti source. In the XRD pattern of CNTs/TiH_2-Ni powders (Blue line in Fig. 2e), the sharp peaks at 2θ=44.5°, 51.8° and 76.4° are attributed to peak positions of Ni with the face-centered cubic structure. [24] The other peaks in XRD pattern of CNTs/TiH_2-Ni powders are the same as CNTs/TiH_2 powders. It suggests that the CNTs/TiH_2 and Ni powders maintain the original state in the mechanical mixing process.

Next, we examined the graphitic structure of the as-grown CNTs, and Raman spectroscopy was conducted with a 514nm wavelength laser in a spectral range of 1000-2000 cm^{-1}. Fig. 2f shows the Raman spectrum for pure TiH_2, CNTs/TiH_2 and

CNTs/TiH_2-Ni powders, respectively. It indicates that Raman spectrum of the pure TiH_2 powders (Black line in Fig. 2f) does not have any peaks. As shown in Fig. 2f, a typically Raman spectrum of the CNTs/TiH_2 powders (Red line in Fig. 2f) exhibits two characteristic carbon bands corresponding to multi-walled CNTs, which are associated with the disorder induced D-band around 1350 cm^{-1}, and the G-band around 1580 cm^{-1} related to in-plane sp^2 vibrations, respectively.[7, 15, 26] Compared with CNTs/TiH_2-Ni powders (see red line and blue line in Fig. 2f), it can be found that the peak positions and I_D/I_G ratio (the intensity ratio of the D-band to G-band) in Raman result are basically unchanged. This result suggests that the CNTs are not damaged in the mechanical mixing process. In addition, the I_D/I_G ratio of as-grown CNTs in CNTs/TiH_2 powders was calculated to be 0.83, as shown in Fig. 2f. The low I_D/I_G value implies that the as-grown CNTs are mainly composed of well-crystallized graphite, which is in agreement with the TEM observations. Namely, the as-grown CNTs exhibit a few defects and complete structure, which makes a perfect structure. Kuzumaki *et al.*[20] reported that the CNTs with perfect structure did not react with the Ti matrix even under hot-pressing for 2 h at ~1000 ^oC. However, CNTs can easily be damaged during traditional preparations of CNTs-reinforced Ti matrix composite,[10-14, 19, 20] such as high-density surface defect and damaged structural of CNTs. CNTs with the incomplete structure are easy to react with Ti at high temperature.[19, 20] Obviously, the composite will lose the strengthening effect of CNTs. Thus, the obtained CNTs with a perfect structure can improve the mechanical performance of the CNTs-reinforced composite. Compared with traditional methods,[10-14] *in-situ* growth of CNTs at a low temperature by PECVD method could realize the homogeneously dispersed and perfect structure of CNTs within the TiH_2-Ni powders. In this way, it can effectively make CNTs homogeneously disperse into the Ti-based brazing alloys

and avoid the reaction between Ti and CNTs.

In order to prove the effect of CNTs in TiNi brazing alloy, the interfacial microstructure and mechanical properties of the SiO_2-BN/Nb joints brazed by TiNi and CNTs/TiNi brazing alloy were comparatively studied. Fig. 3 shows the typical interfacial microstructure of the SiO_2-BN/Nb joint brazed with the TiNi and 1.5vol.%-CNTs/TiNi brazing alloy at 1140 ^oC for 5 min. It is obvious that the joints are soundly bonded without cracks and voids, as shown in Fig. 3a and 3c. In the TiNi brazing alloy, three characteristic zones can be distinguished in the SiO_2-BN/Nb brazed joint, as shown in Fig. 3a and 3b. The brazing alloy reacted with Nb substrate, and thus a continuous ternary eutectic area was formed (denoted by Layer I). A reaction layer (denoted by Layer III) with a thickness of 15μm formed adjacent to the SiO_2-BN substrate. The wide gray reaction layer (denoted by Layer II) with a thickness of 123μm formed in the region between Layer I and Layer III. EDS compositional analyses were performed on each layer in Fig. 3 to identify the possible phases that were presented in the joints. Based on the EDS results in Table 1, the body of a brazed joint was primarily composed of (Nb,Ti) eutectics and TiNi (Points A and B in Layer I), TiNi phase (Point C in Layer II), and TiN, Ti_3O_5 and Ti_5Si_3 compounds (Points E and F in Layer III). According to the previous research[28], it is suggested that Layer I is mainly composed of TiNi-(Nb,Ti) eutectics. Namely, the typical microstructure of the SiO_2-BN/Nb joint brazed with TiNi brazing alloy at 1140 ^oC for 5 min was SiO_2-BN/ TiNi-(Nb,Ti)/TiNi/TiN+Ti_3O_5+Ti_5Si_3/Nb.

In the 1.5vol.%-CNTs/TiNi brazing alloy, the microstructure of the brazed joint is significantly different from that of with the TiNi brazing alloy, as shown in Fig. 3c and 3d. It can be observed that the SiO_2-BN/Nb joint brazed by the CNTs/TiNi brazing alloy mainly consists of one reaction layer, which is composed of TiNi-(Nb,Ti)

eutectics (micro-zone D), as shown in Fig. 3c and Table 1. Namely, the typical microstructure of the SiO_2-BN/Nb joint brazed with CNTs/TiNi brazing alloy at 1140 ^oC for 5 min was SiO_2-BN/TiNi-(Nb,Ti)/Nb. Obviously, the reaction layer (TiNi-(Nb,Ti) eutectics) played a key role in reducing the residual stress and reinforcing the quality of joint. Compared with TiNi brazing alloy (see Fig. 3a and 3c), it can be clearly found that the interface microstructure of the brazed joint has undergone significant changes with some CNTs added into the TiNi brazing alloy. In addition, the main composition of the only reaction layer is similar to Layer I in the reaction layer of the joint brazed with TiNi brazing alloy. Similarly, the reaction layer was formed by reacting between the brazing alloy and Nb, and a ternary eutectic area was formed by dissolution and diffusion of the Nb as the Layer I. The thickness (~235μm) of the reaction layer (TiNi-(Nb,Ti) eutectics) is larger than that (~45μm) brazed without CNTs. It indicates that a small amount of CNTs added into the brazing alloy can significantly increase the diffusing distance of Nb in the brazed joint. Thus, this result suggests that CNTs play a key role in improving the dissolution and diffusion of Nb in the brazed joint.

Considering its applications under high temperatures, it is necessary to analyze the mechanical properties of SiO_2-BN/Nb brazing joints at high temperatures. The shear strengths were tested at both room temperature and high temperatures, as shown in Fig. 4. The average shear strength of the joints brazed using CNTs/TiNi brazing alloy reached 85MPa at room temperature, which was about 70% higher than that (49MPa) of joints brazed with TiNi brazing alloy. It is worth noting that the average shear strength of joints brazed with CNTs/TiNi brazing alloy decline slightly with increasing temperatures. Notably, the average shear strength of joints using CNTs/TiNi brazing alloy was 51MPa (800 ˚C), nearly 170% higher than that (19MPa)

brazed with TiNi brazing alloy. In contrast, the average shear strengths obtained from TiNi brazing alloy was significantly decreased as temperatures increased (see Fig. 4), especially at 800 ^{o}C. Thus, these results suggest that the CNTs played a key role in effectively improving the mechanical performances of brazed joints.

Fig. 5a-d shows the fracture surface of SiO_2-BN/Nb joint after carrying out shear tests at room temperature and high temperature (800 ^{o}C). In the shear tests at room temperature, crack of the joint brazed with TiNi brazing alloy propagated in SiO_2-BN substrate near the braze interface, and a bowed crack path was observed, as shown in Fig. 5a. It indicated that a high residual stress was generated in the SiO_2-BN ceramic resulting in a relatively-low joint strength. Different fracture modes were observed in the joints brazed with CNTs/TiNi brazing alloy, as shown in Fig. 5b. The fracture initiation took place at the reaction layer, and then crack propagated in the SiO_2-BN substrate. So, a step-like fracture surface formed during shear test at room temperature. According to previous reports, [26, 27] the change of the fracture modes suggested that the residual stress was effectively reduced when CNTs were added into the TiNi brazing alloy. In addition, Fig. 5e is an SEM image of the fracture surface in the joint brazed with CNTs/TiNi brazing alloy (corresponding circular area in Fig. 5b), which shows CNTs with an obviously tubular structure. This result suggests that the CNTs with a perfect structure did not react with the Ti at high temperature as 1140 ^{o}C, as demonstrated by Kuzumaki *et al.*[20] Moreover, it can be observed that the CNTs are dispersed very well into the TiNi brazing alloy, and some CNTs are pulled out or broken, which indicates that the load transfer from the brazing alloy to the nanotubes is sufficient to fracture the nanotubes.[21]

In the shear tests at high temperature (800 ˚C), it can be found that the fracture modes of the SiO_2-BN/Nb joint brazed using TiNi and CNTs/TiNi brazing alloy are

substantially the same, as shown in Fig. 5c and 5d. Namely, crack of the joint propagated in the reaction layer, and the fracture surface took place at the reaction layer. Thus, the mechanical properties of the joints are significantly dependent on the reaction layer at high temperature because cracking joints start in the reaction layer under load of high temperature. Combined with the shear strength of joints at 800 ^{o}C (see Fig. 4), it can be found that shear strengths of the joint can be significantly improved by adding some CNTs into the brazing alloy. In the final analysis, some CNTs added into the brazing alloy can significantly increase the mechanical properties of the reaction layer in the fracture area at high temperature.

Based on the above results, it suggests that the CNTs play a key role in two major aspects as reducing residual stress and reinforcing mechanical properties of the brazed joint both at room and high temperatures. In order to reveal the strengthening mechanism of the CNTs in the brazed joint, we conducted the following discussion. On the one hand, it is known that a robust ceramic-metal joint is not only dependent on the strong interfacial bond between ceramic and metal, but also on the favorable stress gradient formed in the joint.[27] Some studies have been performed for a ceramic-metal joint, confirming that there is a high residual stress gradient around the ceramic-metal interface.[27, 29-32] A low joint strength will be unavoidable if the residual stress is not effectively relaxed. Such phenomenon is caused primarily by the significant difference in the CTE between ceramics and metals or brazing alloys. [26, 27] Consequently, it should be noted that the residual stress yielded during cooling due to CTE mismatch between the SiO_2-BN ceramic ($CTE_{SiO2\text{-}BN}$=~1.7×10^{-6}/K) and Nb (CTE_{Nb}=~7×10^{-6}/K) or TiNi brazing alloy (CTE_{TiNi}=~15.4×10^{-6}/K). [27, 33, 34] In our case, the homogeneously dispersed CNTs in the brazing seam of SiO_2-BN/Nb joint resulted from homogeneous dispersion of CNTs in TiNi brazing alloy. The CNTs have

a very low CTE (CTE_{CNTs} =-5.86×10^{-9}/K) [20, 35] values in the brazing seam, and the ability of well bonded CNTs can effectively constrain the expansion of TiNi matrix, [20] which could reduce the CTE of the brazing seam.[27] In addition, the CNTs in the brazing seam could improve the dissolution and diffusion of Nb in the reaction layer of the brazed joint, because it can be beneficial to the homogeneously distribution of Nb in all the brazing seam. Similarly, the Nb has a relatively low CTE value in the brazing seam, which could also reduce the CTE of the brazing seam. Taken together, it is beneficial to reduce joint residual stress because the CTE mismatch between the SiO_2-BN ceramic ($CTE_{SiO2\text{-}BN}$ =~1.7×10^{-6}/K) [27] and the brazing seam was lowered by the addition of CNTs into the brazing alloy. Consequently, the mechanical properties of the brazed joints can be significantly improved by reducing residual stress. On the other hand, it is widely known that the CNTs and Nb have excellent mechanical and high temperature properties.[17, 36, 37] As a result, the homogeneous dispersion of the CNTs and Nb in the brazing seam will effectively improve the mechanical and high temperature properties of the brazed joints. Moreover, the strong interfacial strength between CNTs and TiNi brazing alloy was caused by the better wetting effect of CNTs with Ti and Ni atoms.[38, 39] It is especially important to improve the brazing seam performance because it can cause high load translation during shear process (as suggested by pulling out and broken of CNTs in the inset of Fig. 5e) and thus raise the shear strengths of the brazed joints whether in high or room temperature. Therefore, we believe that the mechanical properties of the brazed joints in both room and high temperature were effectively improved when some CNTs were added into the TiNi brazing alloy.

4. Conclusions

In this paper, we developed a new type of CNTs reinforced TiNi brazing alloy via an

"in-situ growth" mechanism using PECVD, and CNTs with perfect structure are very homogeneously dispersed within the TiNi brazing alloy. The new type of CNTs/TiNi brazing alloy is applied to brazing SiO_2-BN ceramic with Nb. Results show that the introduction of CNTs is very beneficial to the dissolution and diffusion of Nb in the brazed joint. Meanwhile, a homogeneous distribution of CNTs and Nb in the brazing seam could significantly help reduce the residual stress and reinforce mechanical and high temperature properties of the brazed joint. With the 1.5vol.% CNTs added into TiNi brazing alloy, the average shear strength of the brazed joint at room temperature is raised from 49 to 85 MPa, and the average shear strength at 800 ^{o}C (51MPa) is nearly 170% higher than that using TiNi brazing alloy. This study may open the development of CNTs-reinforced brazing alloy in brazing field.

Acknowledgement

The support from the National Natural Science Foundation of China (Grant No 51105108), and the Fundamental Research Funds for the Central Universities (Grant No. HIT. NSRIF. 2010113) is highly appreciated.

References:

1. D. C. Jia, L. Z. Zhou, Z. H. Yang, X. M. Duan and Y. Zhou, *Journal of the American Ceramic Society*, 2011, **94**, 3552.
2. G. Wen, G. L. Wu, T. Q. Lei, Y. Zhou and Z. X. Guo, *Journal of the American Ceramic Society*, 2000, **20**, 1923.
3. Z. W. Yang, L. X. Zhang, X. Y. Tian, Q. Xue and J. C. Feng, *Materials Science & Engineering A*, 2012, **556**, 722.
4. J. Cao, H.Q. Wang, J.L. Qi, X.C. Lin and J.C. Feng, *Scripta Materialia*, 2011, **65**, 261.
5. Z. W. Yang, L. X. Zhang, W. Ren, Q. Xue, P. He and J. C. Feng, *Materials Science & Engineering A*, 2013, **560**, 817.
6. G. B. Lin, J. H. Huang and H. Zhang, *Journal of Materials Processing Technology*, 2007, **189**, 256.
7. Y. M. He, J. Zhang, Y. Sun and C.F. Liu, *Journal of the European Ceramic Society*, 2010, **30**, 3245.
8. B. S. S. Daniel, V. S. R. Murthy and G. S. Murty, *Journal of Materials Processing Technology*, 1997, **68**, 132.
9. M. X. Yang, T. S. Lin, P. He and Y. D. Huang, *Materials Science and Engineering A*, 2011, **528**, 3520.
10. S. M. L. Nai, J. Wei and M. Gupta, *Materials Science and Engineering A*, 2006, **423**, 166.
11. S. M. L. Nai, J. Wei and M. Gupta, *Thin Solid Films*, 2006, **504**, 401.
12. Y. D. Han, H. Y. Jing, S. M. L. Nai, L. Y. Xu, C. M. Tan and J. Wei, *Intermetallics*, 2012, **31**, 72.
13. K. M. Kumar, V. Kripesh and A. A. O. Tay, *Journal of Alloys and Compounds*,

2008, **455**, 148.

14. K. M. Kumar, V. Kripesh and A. A. O. Tay, *Journal of Alloys and Compounds*, 2008, **450**, 229.
15. W. A. Curtin and B. W. Sheldon, *Materials Today*, 2004, **7**, 44.
16. R. George , K. T. Kashyap, R. Rahul and S. Yamdagni, *Scripta Materialia*, 2005, **53**, 1159.
17. R. S. Ruff and D. C. Lorents, *Carbon*, 1995, **33**, 925.
18. R. K. Shiue, S. K. Wu, Y. T. Chen and C. Y. Shiue, *Intermetallics*, 2008, **16**, 1083.
19. X. Feng, J. H. Sui, W. Cai, and A. L. Liu, *Scripta Materialia*, 2011, **64**, 824.
20. T. Kuzumaki, O. Ujiie, H. Ichinose and K. Ito, *Advanced Engineering Materials*, 2000, **2**, 416.
21. C. N. He, N. Q. Zhao, C. S. Shi, X. W. Du, J. J. Li, H. P. Li and Q. R. Cui, *Advanced Materials*, 2007, **19**, 1128.
22. J. L. Qi, Y. H. Wan, F. Zhang, J. Cao, L. X. Zhang and J. C. Feng, *China welding*, 2013, **22**, 42.
23. D. Y. Kovalev, V. K. Prokudina, V. I. Ratnikov, and V. I. Ponomarev, *International Journal of Self-Propagating High-Temperature Synthesis*, 2010, **19**, 253.
24. C. N. He, N. Q. Zhao, C. S. Shi, X. W. Du and J. J. Li, *Materials Letters*, 2007, **61**, 4940.
25. T. M. Marceloa, V. Livramentoa, M. V. Oliveirab and M. H. Carvalhoa, *Materials Research*, 2006, **9**, 65.
26. J. W. Park, P. F. Mendez and T. W. Eagar, *Acta Materialia*, 2002, **50**, 883
27. Z. W. Yang, L. X. Zhang, W. Ren, M. Lei and J. C. Feng, *J Eur Ceram Soc*, 2013, **33**, 759.

28. Y. Z. Liu, L. X. Zhang, C. B. Liu, Z. W. Yang, H. W. Li and J. C. Feng, *Science and Technology of Welding and Joining*, 2011, **16**, 193.

29. C. H. Hsueh and A. G. Evans, *J Am Ceram Soc*, 1985, **68**, 241.

30. A. Abed, P. Hussain, I. S. Jalham and A. Hendry, *J Eur Ceram Soc*, 2001, **21**, 2803.

31. H. Y. Yu, S. C. Sanday and B. B. Rath, *J Am Ceram Soc*, 1993, **76**, 1661.

32. S. B. Lee and J. H. Kim, *J Mater Process Tech*, 1997, **67**, 167.

33. T. Ikeshoji, T. Tokunaga, A. Suzumura and Y. Takahisa, *International Symposium on Interfacial Joining and Surface Technology*, 2014, **61**, 5.

34. Y. Q. Fu and H. J. Du, *Surface and Coatings Technology*, 2002, **153**, 100.

35. R. B. Pipes and P. Hubert, *Composites Science and Technology*, 2003, **63**, 1571.

36. T. Tsuchida and T. Kakuta, *Journal of the European Ceramic Society*, 2007, **27**, 527.

37. C. L. Yeh and W. H. Chen, *Journal of Alloys and Compounds*, 2006, **422**, 78.

38. J. Y. Guo and C. X. Xu, *Applied Physics A*, 2011, **102**, 333.

39. Y. He, J. Y. Zhang, Y. Wang and Z. P. Yu, *Applied physical letters*, 2010, **96**,1.

Table 1. Average chemical compositions of each reactant (at. %) in Fig. 3.

	Ti	Ni	Nb	Si	O	N	Possible phase
A	17.94	6.93	72.97	2.16	—	—	(Nb, Ti)
B	44.45	42.66	11.44	1.45	—	—	TiNi
C	44.25	47.46	6.97	1.33	—	—	TiNi
D	37.82	33.14	27.77	1.26	—	—	TiNi-(Nb,Ti)
E	44.20	4.89	1.50	12.20	6.25	21.78	TiN+Ti_5Si_3
F	48.65	1.21	3.76	2.19	13.54	33.08	TiN+Ti_3O_5

Figure captions:

Figure 1 Schematic of the formation process of CNTs/TiNi brazing alloy.

Figure 2 SEM images of (a) TiH_2, (b, c) CNTs/TiH_2 and (d) CNTs/TiH_2-Ni particles. The inset of (c) is TEM image of the obtained CNTs. (e) XRD pattern and (f) Raman spectra for the CNTs/TiH_2 powders.

Figure 3 SEM images for the typical interfacial microstructure of the BN-SiO_2/Nb joint brazed with (a, b) TiNi and (c, d) 1.5vol.%-CNTs/TiNi brazing alloy at 1140 ^oC for 5 min.

Figure 4 The shear strengths were tested both at room temperature and high temperatures (600 and 800 ^oC).

Figure 5 The fracture surface of SiO_2-BN/Nb joint after carrying out shear tests at (a, c) room temperature and (b, d) high temperature (800 ^oC). (e) SEM image of the fracture surface in the joint brazed with CNTs/TiNi brazing alloy corresponding circular area in (b).

Joining of SiO_2-BN ceramic to Nb using CNTs-reinforced brazing alloy

Jun Lei Qi*, Jing Huang Lin, Yu Han Wan, Li Xia Zhang, Jian Cao, Ji Cai Feng*

State Key Laboratory of Advanced Welding and Joining, Harbin Institute of Technology, Harbin 150001, China

*Corresponding author: Tel. /fax: 86-451-86418146;

E-mail: jlqi@hit.edu.cn (J. L. Qi), fengjc@hit.edu.cn (J. C. Feng);

Figure captions:

Figure 1 Schematic of the formation process of CNTs/TiNi brazing alloy.

Figure 2 SEM images of (a) TiH_2, (b, c) CNTs/TiH_2 and (d) CNTs/TiH_2-Ni particles. The inset of (c) is TEM image of the obtained CNTs. (e) XRD pattern and (f) Raman spectra for the CNTs/TiH_2 powders.

Figure 3 SEM images for the typical interfacial microstructure of the BN-SiO_2/Nb joint brazed with (a, b) TiNi and (c, d) 1.5vol.%-CNTs/TiNi brazing alloy at 1140 ^oC for 5 min.

Figure 4 The shear strengths were tested both at room temperature and high temperatures (600 and 800 ^oC).

Figure 5 The fracture surface of SiO_2-BN/Nb joint after carrying out shear tests at (a, c) room temperature and (b, d) high temperature (800 ^oC). (e) SEM image of the fracture surface in the joint brazed with CNTs/TiNi brazing alloy corresponding circular area in (b).

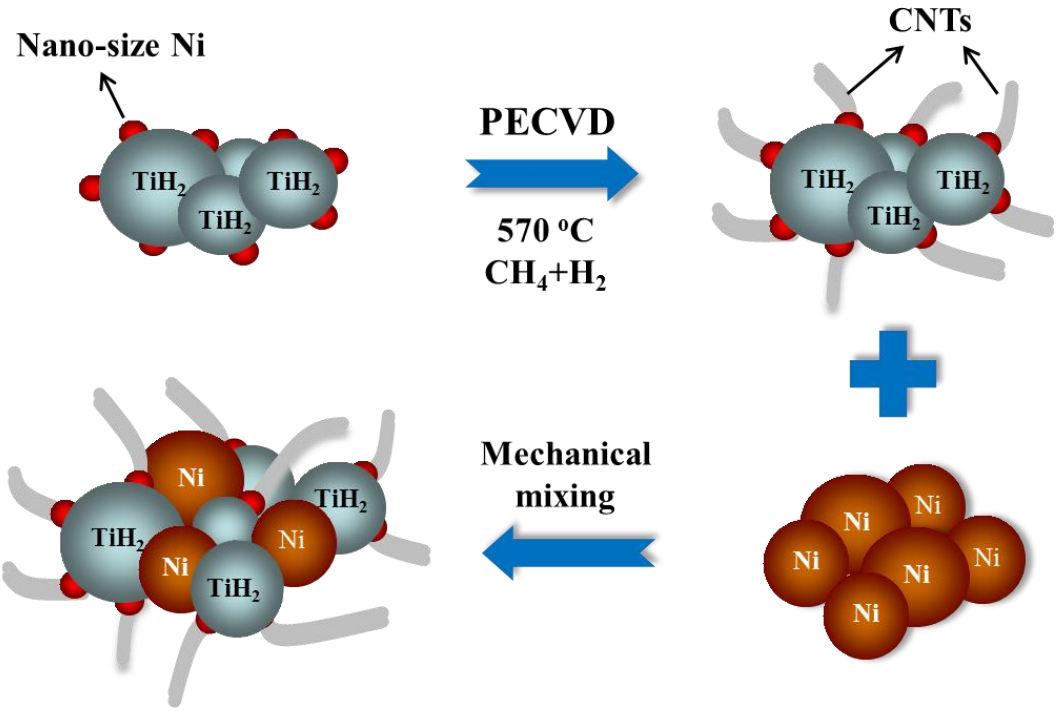

Fig. 1

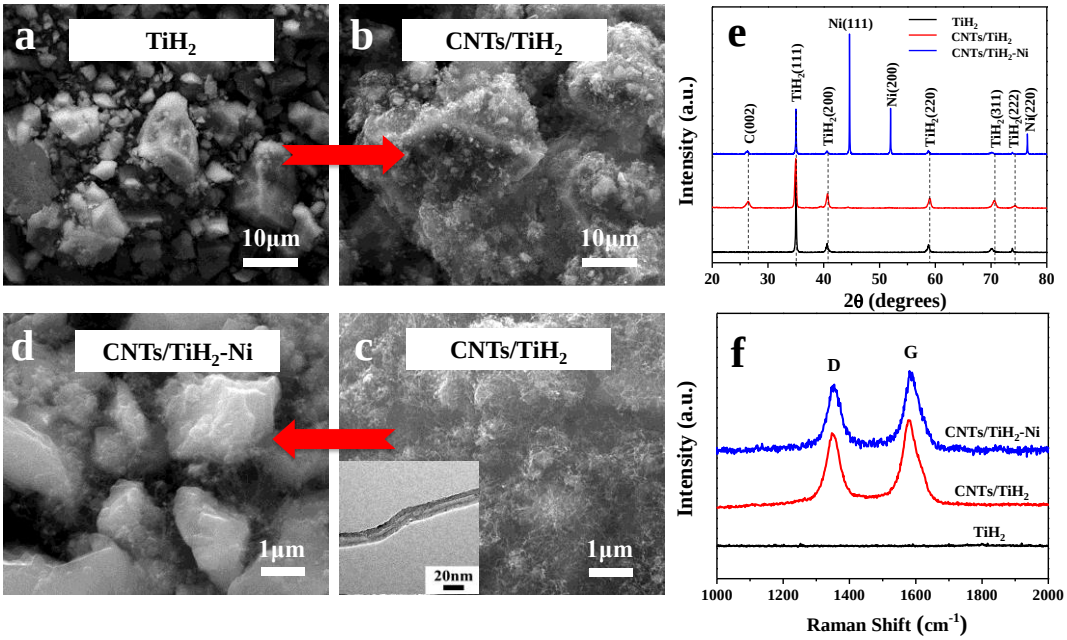

Fig. 2

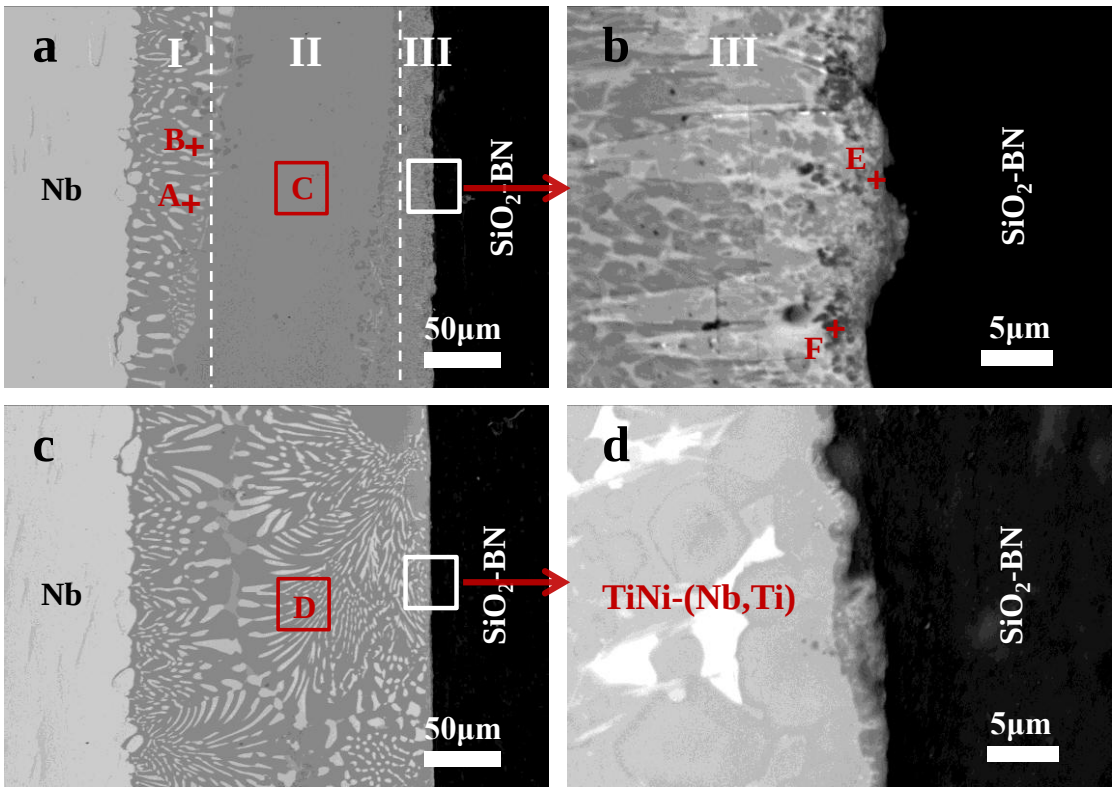

Fig. 3

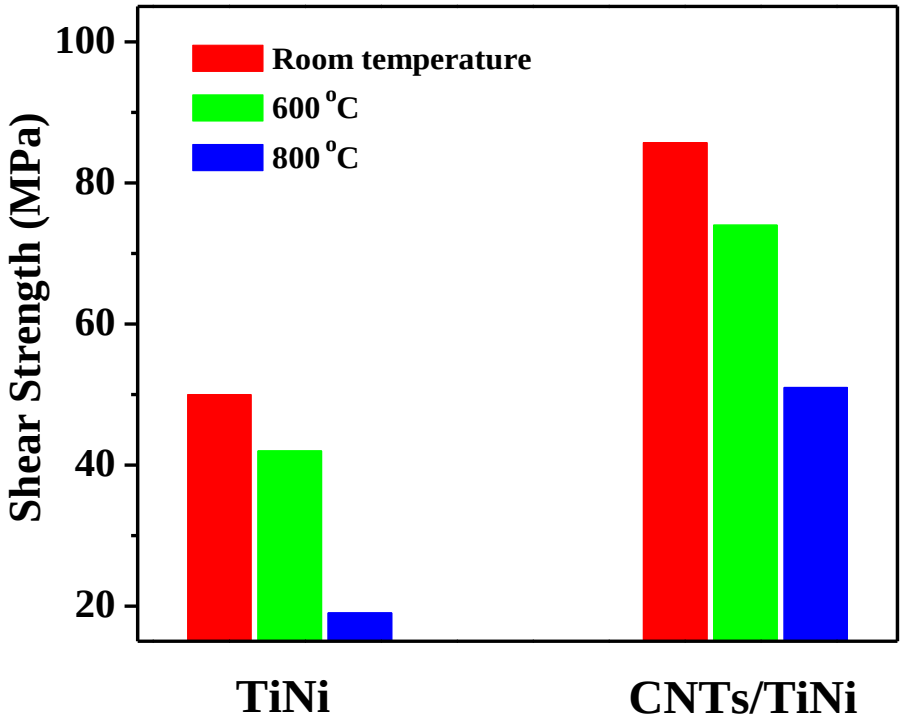

Fig. 4

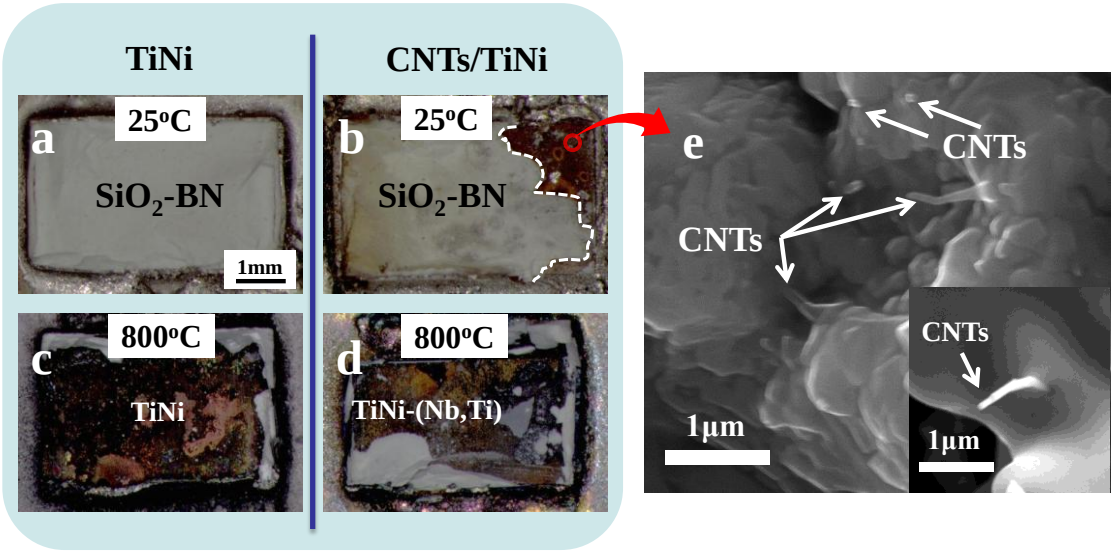

Fig. 5